

## Magic Rule for $Al_nH_m$ Magic Clusters

B. Kiran,<sup>1,\*</sup> P. Jena,<sup>1</sup> X. Li,<sup>2</sup> A. Grubisic,<sup>2</sup> S. T. Stokes,<sup>2</sup> G. F. Ganteför,<sup>2</sup> K. H. Bowen,<sup>2</sup> R. Burgert,<sup>3</sup> and H. Schnöckel<sup>3</sup>

<sup>1</sup>Physics Department, Virginia Commonwealth University, Richmond, Virginia 23284, USA

<sup>2</sup>Departments of Chemistry and Materials Science, Johns Hopkins University, Baltimore, Maryland 21218, USA

<sup>3</sup>Institute of Inorganic Chemistry, University of Karlsruhe (TH), 76128 Karlsruhe, Germany

(Received 24 January 2007; published 20 June 2007)

Using the electronic shell closure criteria, we propose a new electron counting rule that enables us to predict the size, composition, and structure of many hitherto unknown magic clusters consisting of hydrogen and aluminum atoms. This rule, whose validity is established through a synergy between first-principles calculations and anion-photoelectron spectroscopy experiments, provides a powerful basis for searching magic clusters consisting of hydrogen and simple metal atoms.

DOI: 10.1103/PhysRevLett.98.256802

PACS numbers: 73.22.-f, 71.15.Mb, 79.60.-i

Small atomic clusters consisting of less than hundred atoms constitute a metastable form of matter whose properties are size and composition specific and where every atom and electron count. One of the striking properties of atomic clusters is that some of these are unusually stable and appear as conspicuous peaks in the mass spectra [1]. These clusters, commonly referred to as magic clusters, have been a subject of considerable interest not only because they can form the building blocks of a novel class of cluster assembled materials [2], but also an understanding of their stabilities has great scientific significance. However, attempts for a systematic search for their existence have been limited [3].

In this Letter we propose an electron counting rule that enables us to predict the size, composition, and atomic structure of many magic clusters consisting of hydrogen and aluminum atoms. The validity of this rule is established by a synergistic approach involving density functional theory and anion-photoelectron spectroscopy experiment. The agreement leads us to believe that this rule may be useful in generating a large number of magic clusters hitherto unknown and guide experimentalists in their discoveries. Materials composed of these magic clusters may have applications as hydrogen storage and high energy-density materials.

We have chosen aluminum-hydrogen clusters ( $Al_nH_m$ ,  $n > m$ ) for the following reasons: (a) aluminum is a simple metal where the valence electrons are nearly free and the electronic structure can be described by the Jellium model. More than two decades ago, Knight *et al.* [1] showed that nearly free electron Na clusters consisting of 2, 8, 20, 40, ... atoms are unusually stable compared to their neighbors and attributed the origin of their stability to the successive electronic shell closure of  $1s^2$ ,  $1p^6$ ,  $1d^{10}$ ,  $2s^2$ ,  $1f^{14}$ ,  $2p^6$ , ... quantized levels, much the same way as nuclear shell closure gave rise to magic nuclei. The stability of certain Al clusters can be explained from the above electronic shell closure argument. For example,  $Al_7^+$  and  $Al_{13}^-$  clusters containing 20 and 40 electrons, respectively, are known to be magic [4]. (b) Hydrogen, on the other hand, is a unique element in the periodic table. In addition to being

the lightest element, it has a high ionization potential (13.6 eV) and significant electron affinity (0.75 eV). These properties render hydrogen some of the most fascinating physical and chemical properties. The ability of hydrogen to share, donate, or accept an electron gives rise to a variety of bonding characteristics ranging from covalent ( $H_2$  and organic molecules), ionic (LiH), metallic (intermetallic hydrides), to weak hydrogen bonds (proteins). We believe that this flexibility of hydrogen to form various types of bonds can be utilized to design  $Al_nH_m$  clusters with magic properties. We note that hydrogen atoms can bind to an  $Al_n$  cluster either on the radial (on top site) or bridge sites and the choice would be dictated by whatever minimizes the total energy. We further note that in the radial position, hydrogen would form a covalent bond with the Al atom while in the bridge bonded case, hydrogen's electron would become delocalized. (c) The nature of bonding and structure of  $Al_nH_m$  clusters in the Al rich phase ( $n \gg m$ ) is expected to be different from that in the H rich phase ( $n \ll m$ ): while in the latter covalent bonding is likely to dominate, it is in the former that the electronic structure of the cluster may be described in terms of a free electron or Jellium model.

We focus on the Al rich phase of  $Al_nH_m$  clusters, namely  $n/m \geq 2$ . We begin with the following two hypotheses: (1) hydrogen's contribution to the total valence electron count in an  $Al_nH_m$  cluster would depend upon whether the H atom is bound to a single Al atom radially or to two or more Al atoms on the bridge or face sites. In the former case, the Al-H pair can only donate 2 electrons as two of the four valence electrons of the Al-H pair are localized in the covalent bond. On the other hand, in the latter case each H and Al atom can donate 1 and 3 electrons, respectively. Thus, an  $Al_nH_m$  cluster can be written as  $Al_{n-i}(AlH)_iH_{m-i}$ , where  $i$  represents the number of radial Al-H bonds. Then  $(n-i)$  is the number of nonradially bonded Al atoms and  $(m-i)$  is the number of bridge bonded H atoms. Since  $i$  number of Al-H units,  $(n-i)$  number of Al atoms, and  $(m-i)$  number of H atoms contribute, respectively, 2, 3, and 1 electron each, the total number of valence electrons,  $N$ , responsible for the binding of the  $Al_nH_m$  cluster is then

given by

$$N = 3(n-i) + 2i + (m-i) = 3n - 2i + m, \quad (1)$$

$$i \leq n \quad \text{and} \quad i \leq m.$$

Note that  $i$  (the number of radially bonded H atoms) cannot exceed either  $n$  (the number of Al atoms) or  $m$  (the total number of H atoms) in the  $\text{Al}_n\text{H}_m$  cluster. (2) For a given  $n$  the number of radial H atoms  $i$  should be such that the total number of valence electrons,  $N$ , determined via Eq. (1), matches one of the Jellium model predicted numbers for electronic shell closure ( $N = 2, 8, 18, 20, 34, 40, \dots$ ). The electronic stability gained by the shell closure in these magic clusters is, therefore, the driving force for hydrogen selecting between the bridging and radial sites.

In the following, we discuss results of  $\text{Al}_n\text{H}_m$  clusters consisting of  $n \geq 6$  Al atoms, since it has been demonstrated earlier [4] that  $s$ - $p$  hybridization in small Al clusters does not set in until  $n \geq 6$ . In Table I we list all possible values of  $n$ ,  $i$ , and  $m$  predicted by Eq. (1) for  $N = 20$ , when the previously mentioned constraint that  $n/m \geq 2$  is taken into account. For  $N = 40$ , we only list two representative clusters, although many more clusters obeying Eq. (1) can be easily generated. The fifth column of Table I lists the corresponding formulas of  $\text{Al}_n\text{H}_m$  clusters that should be magic according to our hypotheses. In the fourth column, we indicate the number of radially bonded H atoms that are necessary for electronic shell closure, thus illustrating the likely arrangement of hydrogen atoms in these magic clusters. The validity of the predictions in Table I is first established by determining independently the ground state geometries and binding energies of these  $\text{Al}_n\text{H}_m$  clusters from calculations based on density functional theory and PW91 form for the exchange correlation functional. We have used the triple zeta valance polarization basis for the atomic orbitals of Al and H and the GAUSSIAN 03 suite of programs for all our calculations [7]. The geometries were optimized by using different initial configurations and without any symmetry restrictions. The energies and forces at every atom site were converged to 0.00001 eV and 0.001 eV/Å, respectively. As shown below, in all cases studied the predictions of the rule in Eq. (1) are validated. We have also calculated the structures and total energies of low lying isomers by mov-

ing H atoms away from the position predicted by our rule, and the results demonstrate that all of these isomers are indeed *higher* energy structures. Note that Eq. (1) predicts the number of radial and bridge bonded hydrogen atoms but does not illustrate, among all possible radial and bridge sites, which particular sites may be preferred. Thus in our geometry optimization process we have examined all possibilities and only discuss the low lying isomers in this Letter.

We first discuss the geometries of neutral  $\text{Al}_n\text{H}_m$  clusters containing 6, 7, and 8 Al atoms corresponding to the  $N = 20$  electron system. The ground state and low lying isomers of these clusters are given in Fig. 1. Note that the ground state geometries of  $\text{Al}_6\text{H}_2$ ,  $\text{Al}_7\text{H}$ ,  $\text{Al}_7\text{H}_3$ , and  $\text{Al}_8\text{H}_4$  clusters contain 0, 1, 2, and 4 radially bonded H atoms, respectively—in exact agreement with the numbers predicted by the proposed rule (fourth column of Table I). The geometries of the lowest lying isomers of each species are also given in Fig. 1 along with their relative energies calculated with respect to the ground state geometries. These isomers lie between 0.23 eV and 1.16 eV above the ground state structures. The calculated highest occupied molecular orbital–lowest unoccupied molecular orbital (HOMO-LUMO) gaps ( $\epsilon_{\text{LUMO}} - \epsilon_{\text{HOMO}}$ ) of the neutral  $\text{Al}_6\text{H}_2$ ,  $\text{Al}_7\text{H}$ ,  $\text{Al}_7\text{H}_3$ , and  $\text{Al}_8\text{H}_4$  clusters are 1.53, 1.70, 1.37, and 1.45 eV, respectively. To put this in perspective we note that the experimentally determined HOMO-LUMO gap of  $\text{Al}_{13}\text{K}$ , a well-established magic cluster, is 1.29 eV [8]. Next, we focus on two representatives of the 40-electron systems—neutral  $\text{Al}_{13}\text{H}$  and  $\text{Al}_{14}\text{H}_2$  clusters (Fig. 1). Calculated structures again exactly match the predictions of Eq. (1) summarized in Table I. The ground state structure of  $\text{Al}_{13}\text{H}$  has the H atom in a bridging position while in the ground state of  $\text{Al}_{14}\text{H}_2$ , both atoms are radially bonded. The isomers of  $\text{Al}_{13}\text{H}$  with radially bonded H and that of  $\text{Al}_{14}\text{H}_2$  with one radially bonded and one bridge bonded H are 0.29 eV and 0.36 eV, respectively, higher in energy than the ground state structures. The calculated, large HOMO-LUMO gaps of  $\text{Al}_{13}\text{H}$  (1.87 eV) and  $\text{Al}_{14}\text{H}_2$  (1.29 eV), indicative of their enhanced stability, are consistent with the predictions of our proposed magic rule. Thus, it is remarkable that the ground state of all these clusters with varying number of Al and H atoms have one property in common—they all have either 20 or

TABLE I. Composition of magic clusters having the stoichiometry  $\text{Al}_{n-i}(\text{AlH})_i\text{H}_{m-i}$ .

# of electrons	$n$	$m$	$i$	Stoichiometry	ADE		HOMO-LUMO gap	
					Theory	Experiment	Theory	Experiment
20	6	2	0	$\text{Al}_6\text{H}_2$	1.76	$1.66 \pm 0.15$ , Ref. [5]	0.68	$1.0 \pm 0.10$ , Ref. [5]
20	7	1	1	$\text{Al}_7\text{H}$	1.88 <sup>a</sup>	$1.85 \pm 0.05$	0.81	$1.2 \pm 0.1$
20	7	3	2	$\text{Al}_7\text{H}_3$	2.01	$2.0 \pm 0.20$	0.49	$0.4 \pm 0.2$
20	8	4	4	$\text{Al}_8\text{H}_4$	1.93 <sup>a</sup>	$1.95 \pm 0.05$	0.70	$0.8 \pm 0.1$
40	13	1	0	$\text{Al}_{13}\text{H}$	1.99	$2.0 \pm 0.05$ , Ref. [6]	1.12	$1.4 \pm 0.20$ , Ref. [6]
40	14	0	2	$\text{Al}_{14}\text{H}_2$	2.34 <sup>a</sup>	$2.4 \pm 0.10$ , Ref. [6]	0.78	$0.75 \pm 0.25$ , Ref. [6]

<sup>a</sup>Values also represent  $\text{EA}_a$  values.

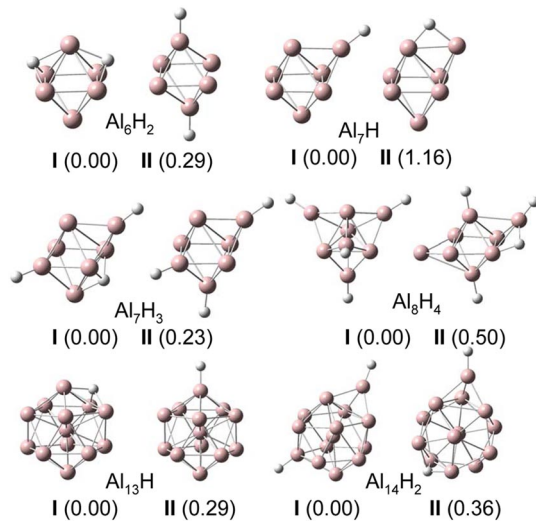


FIG. 1 (color online). Computed geometries of two low lying isomers of representative  $\text{Al}_n\text{H}_m$  ( $n > m$ ) clusters along with their relative energies (eV).

40 delocalized electrons. Because of the electronic shell closure, they all have large HOMO-LUMO gaps and can, therefore, be classified as magic clusters.

To establish the validity of our theoretical conclusions, we compare our calculated HOMO-LUMO gaps of the neutrals and adiabatic detachment energies (ADE) of the corresponding anions with the experimental values obtained from the anion-photoelectron spectroscopy. The technique and details of our apparatus have been presented elsewhere [9,10]. Briefly, the pulsed arc discharge source [6,11] was employed to generate  $\text{Al}_n\text{H}_m^-$  clusters. The electrons ejected during a photo-detachment event with a fourth harmonic (266 nm, 4.661 eV) Nd:YAG laser were analyzed by a magnetic bottle electron analyzer that has a resolution of 35 meV at 1 eV electron kinetic energy.

The onset of the lowest electron binding energy feature in the photoelectron spectra represents the minimum energy required to strip the electron off the probed anion. This ADE is defined as the energy difference between a particular anion and its corresponding neutral at the relaxed anion geometry. Note that the quantity is defined for every anion species, regardless of whether it is a ground state or higher energy isomer, and it is the most useful quantity to compare measured photoelectron spectra with the calculations. In a particular case, when the anion is in its ground state and the resulting neutral is also a ground state isomer, the quantity is interpreted as adiabatic electron affinity ( $\text{EA}_a$ ). Fortunately, the latter case is most commonly encountered in anion-photoelectron spectroscopy and allows for the determination of this fundamental property of the neutrals. Anion-photoelectron spectroscopy also provides information about HOMO-LUMO gaps of the neutral clusters. In a neutral cluster with closed shell, the additional electron occupies the LUMO of the corresponding neutral. This extra electron has a low binding energy, followed by an energy gap. Thus the anion-

photoelectron spectroscopy provides the measure of the HOMO-LUMO gap of the corresponding neutral cluster provided the geometries of the anion and neutral clusters do not differ much. However, great many binding sites on the surface of the aluminum cluster, where hydrogen can bind, lead to a myriad of local minima structures for the neutral as well as the anion. This could potentially lead to a situation where the generated ground state anion produces a higher energy neutral isomer upon photodetachment that does not show a characteristic HOMO-LUMO gap predicted for the neutral ground state. It, indeed, turns out that while the neutral  $\text{Al}_n\text{H}_m$  clusters adopt geometries (Fig. 1) that follow the proposed electron counting rule, the anions rather adopt geometries where hydrogen preferentially binds via radial bonds, as demonstrated in Fig. 2. The shown optimized structures of  $\text{Al}_n\text{H}_m^-$  clusters were obtained using the same procedure as outlined above for the neutrals. In order to adequately compare experiment with the theoretical predictions, the photoelectron spectra of only those anions need to be considered, whose geometry resembles that of the predicted ground state neutrals. Only  $\text{Al}_7\text{H}^-$ ,  $\text{Al}_8\text{H}_4^-$ , and  $\text{Al}_{14}\text{H}_2^-$  species with all radial hydrogen atoms show such resemblance in their ground states. For the remaining three,  $\text{Al}_6\text{H}_2^-$ ,  $\text{Al}_7\text{H}_3^-$ , and  $\text{Al}_{13}\text{H}^-$ , however, one would have to generate a higher energy isomer in order to access the neutral ground state potential energy surface upon photodetachment. Fortunately, access to the pulsed arc discharge source allowed us to produce ground state as well as occasionally higher energy anion isomers [12]. We speculate that by carefully tuning the source conditions one transitions from the most common “born ionic” (i.e., anion clusters relaxes to its ground state geometry after the electron is attached) to the “born neutral” (i.e., electron is attached once the neutral clusters reach their ground state) ion forming regime.

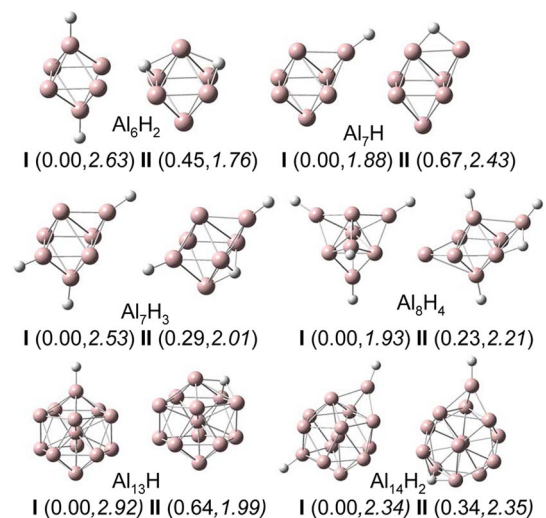


FIG. 2 (color online). Computed geometries of two low lying isomers of  $\text{Al}_n\text{H}_m^-$  clusters. The relative energies and the ADE (in italics) are given in eV.



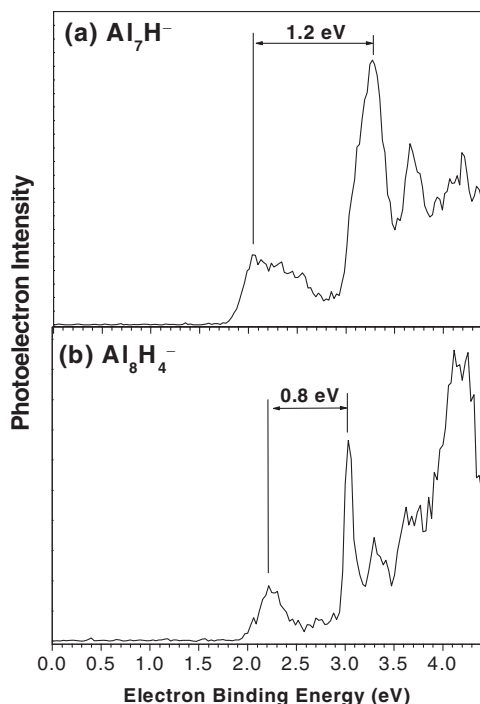


FIG. 3. Photoelectron spectra of (a)  $\text{Al}_7\text{H}^-$  and (b)  $\text{Al}_8\text{H}_4^-$ . Estimated HOMO-LUMO gaps of the corresponding neutrals are marked with horizontal arrows.

We present photoelectron spectra of the two anions,  $\text{Al}_7\text{H}^-$  and  $\text{Al}_8\text{H}_4^-$ , that in their ground state resemble the corresponding neutral ground state the most (Fig. 3). The calculated adiabatic electron affinities of  $\text{Al}_7\text{H}$  (1.88 eV) and  $\text{Al}_8\text{H}_4$  (1.93 eV) are in excellent agreement with our experimental numbers of  $1.85 \pm 0.05$  eV and  $1.95 \pm 0.05$  eV, respectively. Both of them also exhibit significant HOMO-LUMO gaps in agreement with the predicted stabilities of the 20 electron neutral structures (Table I). Photoelectron study on  $\text{Al}_{14}\text{H}_2^-$  done by Gantefoer [6] determined an  $\text{EA}_a$  of  $2.4 \pm 0.1$  eV and a HOMO-LUMO gap of  $0.75 \pm 0.25$  eV, which are in good agreement with the predictions for the 40 electron neutral  $\text{Al}_{14}\text{H}_2$  system (Table I). Of the remaining three studied neutrals,  $\text{Al}_6\text{H}_2$ ,  $\text{Al}_7\text{H}_3$ ,  $\text{Al}_{13}\text{H}$  that necessitate generating higher energy anion isomers in order to probe their electronic structure, we were able to produce the higher energy species of only  $\text{Al}_{13}\text{H}^-$  [12]. The same ion was first observed by Gantefoer [6], who reported an ADE of 1.98 eV. The value matches very well with the calculated value of 1.99 eV predicted for the  $\text{Al}_{13}\text{H}^-$  (II) ( $41e^-$ ) isomer in which H occupies a face site and displays a large HOMO-LUMO gap, consistent with the expected stability of the resulting ground state neutral  $\text{Al}_{13}\text{H}$  ( $40e^-$ ). Although higher energy anion isomers of  $\text{Al}_7\text{H}_3^-$  and  $\text{Al}_6\text{H}_2^-$  were not observed in our studies, the anion-photoelectron spectrum of what appears to be a higher energy isomer of  $\text{Al}_6\text{H}_2^-$  was reported by Wang and co-workers [5]. With a total of 17 cluster electrons, the ground state of  $\text{Al}_6\text{H}_2$  (I)

anion, where both hydrogen atoms are radially bonded to the opposite Al atoms, is very stable compared to the anion derived from the neutral ground state (II), which has 21 electrons. The ADE of both isomers of  $\text{Al}_6\text{H}_2$  were calculated to be 2.63 eV and 1.76 eV, respectively. In addition, if the 17-electron  $\text{Al}_6\text{H}_2$  (I) anion were observed there would be no HOMO-LUMO gap, because its neutral is a triplet. On the other hand, if  $\text{Al}_6\text{H}_2$  (II) anion is observed then there will be a considerable HOMO-LUMO gap. Wang and co-workers have reported the ADE of  $\text{Al}_6\text{H}_2$  to be  $1.66 \pm 0.15$  eV which is in excellent agreement with the predictions about  $\text{Al}_6\text{H}_2^-$  (II) [5]. The good agreement between calculated and experimentally observed values of ADE/ $\text{EA}_a$  and HOMO-LUMO gaps provides support for our theoretical calculations, and hence for the validity of the rule in Eq. (1).

In conclusion, we have provided a simple electron counting rule that enables us to predict the number of radially or bridged bonded H atoms in Al rich  $\text{Al}_n\text{H}_m$  clusters ( $n/m \geq 2$ ). We have demonstrated in these systems that H atoms select between the radial and bridging or face sites on the Al clusters in a way that makes the total number of valence electrons attain electronic shell closure. Several  $\text{Al}_n\text{H}_m$  clusters were predicted to be magic under this rule. Our predictions were verified through both first-principles calculations and anion-photoelectron spectroscopy experiments. The proposed electron counting rule provides a powerful tool for searching new magic  $\text{Al}_n\text{H}_m$  clusters and guide experimentalists in their discoveries. It will be interesting to see if this rule applies only to Al or other simple metals as well.

This work was supported in part by grants from the Department of Energy (P.J.), Air Force Office of Scientific Research (K.B.), and Deutsches Forschungsgemeinschaft (G.G., H.S.).

\*Corresponding author.

Email address: kboggavarapu@vcu.edu

- [1] W.D. Knight *et al.*, Phys. Rev. Lett. **52**, 2141 (1984).
- [2] S.N. Khanna and P. Jena, Phys. Rev. Lett. **69**, 1664 (1992).
- [3] S. Saito and S. Ohnishi, Phys. Rev. Lett. **59**, 190 (1987); H. Häkkinen and M. Manninen, Phys. Rev. Lett. **76**, 1599 (1996); G. Rosenfeld *et al.*, Phys. Rev. Lett. **69**, 917 (1992); B.K. Rao *et al.*, Phys. Rev. Lett. **86**, 692 (2001).
- [4] B.K. Rao and P. Jena, J. Chem. Phys. **111**, 1890 (1999).
- [5] L.F. Cui, X. Li, and L.S. Wang, J. Chem. Phys. **124**, 054308 (2006).
- [6] S. Burkart *et al.*, Chem. Phys. Lett. **301**, 546 (1999).
- [7] M.J. Frisch *et al.*, GAUSSIAN03 (Gaussian, Inc., Pittsburgh, PA, 2004).
- [8] W.J. Zheng *et al.*, J. Chem. Phys. **124**, 144304 (2006).
- [9] M. Gerhards *et al.*, J. Chem. Phys. **116**, 10247 (2002).
- [10] X. Li *et al.*, Science **315**, 356 (2007).
- [11] H.R. Siekmann *et al.*, Z. Phys. D **20**, 417 (1991).
- [12]  $\text{Al}_{13}\text{H}$  in preparation.